

Developable Modes in Vibrated Thin Plates

Arezki Boudaoud

Laboratoire de Physique Statistique, UMR 8550 du CNRS, Ecole Normale Supérieure, Universités Paris VI et Paris VII, 24 rue Lhomond, 75231 Paris Cedex 05, France

Eugenio Hamm and Francisco Melo

Departamento de Física and Center for Advanced Interdisciplinary Research in Materials (CIMAT), Universidad de Santiago de Chile, Avenida Ecuador 3493, Casilla 307, Correo 2, Santiago de Chile
(Received 19 July 2007; published 21 December 2007)

We investigate the normal modes of a developable cone singularity as observed in a circular sheet supported by a rigid circular frame and pushed at its center. When the center of the sheet is in addition submitted to a sinusoidal forcing, two types of bending modes, named here rolling and tilt modes, are parametrically excited. The rolling mode is an angular oscillation of the concave sector of the developable cone structure. If the amplitude of vibration is high enough, the rolling mode amplitude increases dramatically giving rise to both a continuous rotation of the concave sector and a material angular displacement of the sheet, similar to that produced by a moving wrinkle in a carpet.

DOI: [10.1103/PhysRevLett.99.254301](https://doi.org/10.1103/PhysRevLett.99.254301)

PACS numbers: 46.32.+x, 46.40.-f, 46.70.De

The equilibrium configurations of thin-walled objects under large deformation have been described in recent work in terms of robust point and line defects—respectively developable cones [1–3] and ridges [4–6]. These defects play a central role in the process of folding and crumpling of thin sheets, showing universal behavior and cascadelike phenomena (see [7] and references therein). Full dynamical studies are scarce [8]. Sound emission during crumpling of elastic sheets has been also explored, showing a universal power law in the emitted noise [9,10]. The study of propagation of transverse elastic waves in crumpled media [11] suggests that ridges act as barriers to wave propagation and that modes in a certain frequency regime could be trapped in the facets.

Here we focus on the dynamics of a developable cone (d cone). The simplest structure can be obtained by forcing a circular sheet with a stick into a rigid cylindrical hoop of smaller diameter [2,3,12]. Thus, the sheet deforms into a nonsymmetric conical surface, which is in partial contact with the hoop (see Fig. 1); thus the surface is made of two parts: a convex sector which is almost included in a cone of revolution and a concave sector that accommodates the excess in area. The surface is almost singular at the tip, a characteristic feature of a d cone, while the peripheral region is dominated by bending [1,3]. Because of its importance in folding problems and stability of crumpled surfaces, the quasistatic dynamics of d cones has received attention as well. For instance, in a cylindrical arch deformed in the other direction by a load applied at its center, as a result of elastic energy minimization, d cone singularities experience continuous displacement as the load is increased [13,14].

In this Letter we consider the temporal dynamics of d cones. We investigate the frequency response of the simplest structure nucleated in a circular sheet by imposing the

displacement of its center. The sheet is set into motion by an additional vibration of the center. Two oscillatory bending modes of the structure are observed as a function of amplitude and frequency forcing, namely, a tilt (TM) and a rolling mode (RM). The former is an alternating asymmetric tilt of the concave sector of the d cone that can be parametrically coupled to the vertical oscillation. The latter is the angular oscillation of the concave sector of the d cone. Because of the elastic anisotropy of the sheet, two preferential positions exist for which the concave d cone sector minimizes the bending energy, and so around each energy minimum rolling oscillations are made possible. These preferential directions allow to characterize the generic effects on a d cone of any anisotropy, such as those induced by the presence of other defects. For some forcing conditions, the concave sector of the d cone rotates con-

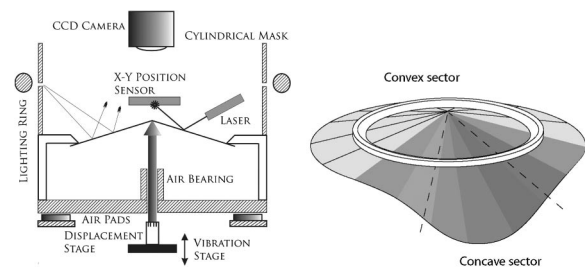


FIG. 1. Sketch of experimental setup. A rigid frame of radius $R = 56$ mm holds a circular sheet, of radius $R_s = 73$ mm, which vertical static deflection d is adjusted by a microdisplacement stage. An oscillatory vertical displacement of amplitude d_F and frequency f is superimposed. A schematic of the sheet shape (developable cone structure) is shown on the right. Shaded region indicates sector of the sheet which is not in contact with the cylindrical hoop (in white), while dashed lines delimit the concave sector.

tinuously. This motion, which is equivalent to that of an edge dislocation in a simple solid or that of a wrinkle on a carpet, produces a global rotation of the sheet. At each turn, the sheet experiences a rotation equal to the angular excess contained in the concave sector. This is reminiscent of the motion of a slip pulse along sheared frictional interfaces as in earthquakes [15], the carpet wrinkle being the analogous to the slip pulse. More generally, the motion of the concave sector of the d cone has common features with particle motion in a fluctuating potential, such as molecular motors [16] or bouncing droplets [17].

Experimental setup.—In all our experiments, a thin circular sheet of radius $R_s = 73$ mm is perpendicularly pushed by a centered finger against a cylindrical rigid frame of inner radius $R = 56$ mm and oriented horizontally (Fig. 1). Such forcing induces the nucleation of an isolated d cone structure [2,3,12]. The strength of the d cone can be quantified with the ratio ϵ between the displacement of the center d and the radius of the hoop R . The circular plate has thickness $h = 0.1$ mm and is cut from a film transparency for printing (3M CG3300), (Young's modulus $E \approx 4.3 \times 10^9$ Pa, Poisson ratio $\nu = 0.4$, and density $\rho = 1400$ kg/m³.) To excite vibrations the sheet is coupled vertically to the end of a vibrating shaft (7 mm diameter) by means of a 0.7 mm screw and a hole 0.8 mm in diameter centered on the plate, providing a low friction coupling and almost free rotation of the sheet. Friction at the rigid frame contact increases with d cone amplitude avoiding any angular sliding of the sheet at the hoop. Vertical vibration of the shaft is achieved by an electromechanical shaker whose acceleration is monitored by a miniature accelerometer (Brüel Kjaer 4374) with a precision better than 0.01 g. A precision function generator provides frequency and amplitude control to the vibration. The shaft, which is relatively flexible, is in turn mounted in a low friction bearing to avoid lateral coupling with the cell frame. The whole cell is mounted on three air pads and kept horizontal in such a way that it is almost free to move laterally. Thus the shaft centers automatically and our setup insures highly pure sinusoidal, vertical excitation of the plate. No lateral vibration was detected with the resolution achieved here. Precise measurements of local vibration of the sheet are carried out by a laser diode beam and a four quadrant position sensor whose sensitive area is 4 cm². Both are located a few centimeters above the plate, according to Fig. 1, and allow to register any change in the local slope of the sheet.

Tilt mode.—Several phenomena are observed when the d cone structure is excited by superimposing an oscillatory disturbance of frequency f and amplitude d_F , on the static deflection d . The general diagram of the sheet response is presented in Fig. 2. At high frequency, a parametric instability of the tilt mode TM is observed with the concave sector of the d cone oscillating at $f/2$ (see the inset of Fig. 2 for a sketch of the TM). Since the TM asymmetri-

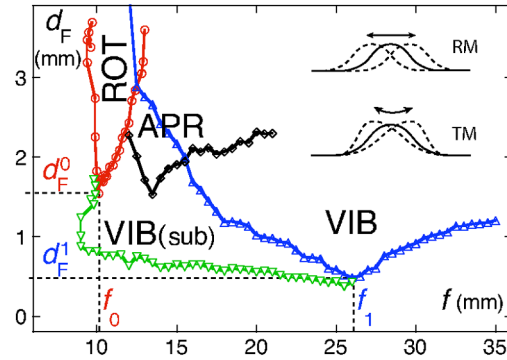


FIG. 2 (color online). Phase diagram as a function of forcing frequency f and forcing amplitude d_F for static center displacement $d = 4$ mm. VIB stands for vibration of the sheet, ROT for rotation of the sheet, and APR for aperiodic rotation. The triangles pointing up correspond to thresholds measured for increasing amplitudes d_F whereas all other symbols were obtained for decreasing amplitudes. Inset: rolling (RM) and tilt modes (TM).

cally modulates curvature (see inset of Fig. 2), at the two edges where the sheet loses contact with the frame, moments have not equal values providing the restoring force for this mode. When vibration is introduced reactions at these edges are modulated affording the mechanism for parametric coupling. As observed from the phase diagram, a lowest threshold d_F^1 for parametric excitation of the TM occurs at frequency f_1 . For f larger than f_1 the parametric oscillation is supercritical showing no hysteresis. In contrast for f lower than f_1 , this transition becomes subcritical showing notorious hysteresis as indicated in the phase diagram by two stability limits, VIB and VIB(sub). The upper and lower curves are obtained for increasing and decreasing forcing amplitude, respectively. We note that such features are the signature of a parametric instability, well established in Faraday waves [18]. We have checked that f_1 is twice the natural frequency ν_1 of the TM. ν_1 was measured by analysis of the free oscillations after the concave d cone region is released from an asymmetric disturbance; by following the laser reflection on the sheet, we found ν_1 in the range 12.5–14.2 Hz, almost independent on static deflection d [see Fig. 3(a)]. Consistently the lower limit f_1 is independent on d cone amplitude and always twice ν_1 , indicating a robust parametric coupling of the bending mode TM with forcing. In turn, d_F^1 increases with d [see Fig. 3(b)] indicating an increase in energy dissipation [18], likely due to the friction of the sheet with the rigid frame.

Rolling mode.—A well-defined continuous rotation RM of the concave sector occurs inside a tongue labeled by ROT in Fig. 2. This rotation was recorded by a high speed video camera centered above the plate. Suitable lighting is provided by a centered fluorescent ring and a cylindrical mask as shown in Fig. 1. Thus, the CCD camera registers images of the reflection of the bright ring on the surface of

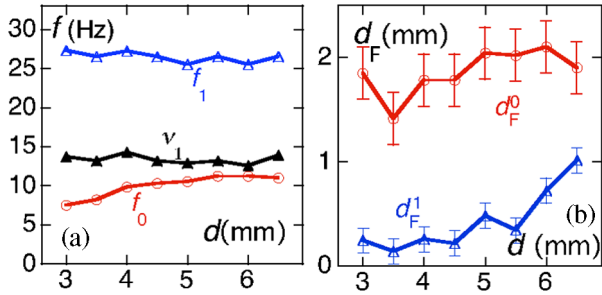


FIG. 3 (color online). Minima of the vibration (VIB) and rotation (ROT) tongues of Fig. 2, as a function of the center static displacement d . (a) Frequencies f_0 (ROT) and f_1 (VIB), and frequency of decaying free oscillations, ν_1 . (b) Thresholds in amplitude of forcing d_F^0 (ROT) and rotation d_F^1 (VIB).

the sample. If the plate were a perfect cone, the registered image would be a circle whose radius would decrease with increasing amplitude of the cone [see Figs. 4(b), 4(d), and 4(f)]. Instead, the characteristic concave region of a d cone deflects the circle inwards, hence giving information on the orientation of the d cone, even at relatively high plate deflection, where images become more complex. Figure 4 shows almost one complete revolution of the concave sector. Coming back to the ROT tongue (Fig. 2), the lowest amplitude threshold d_F^0 occurs at frequency f_0 . The rolling mode RM is coupled parametrically to external vibration as well, its rotation frequency being $f/2$. As seen in Fig. 3(a), f_0 increases slightly with d indicating that the restoring force of RM increases with d cone amplitude as well. The amplitude threshold d_F^1 is almost constant [Fig. 3(b)]. As will be discussed in the theoretical part below, this mode is sensitive to the anisotropy of the sheet. Eventually, we observed aperiodic rolling motion of the d cone (aperiodic rotation tongue, APR, in Fig. 2), characterized by intermittent rolling of the d cone in either direction.

Material rotation.—In the ROT tongue, in addition to the fast wavelike rotation of the concave sector, a slow material rotation of the sheet occurs, with periods of 1 to

5 minutes, as can be seen by following a material radial line drawn on the sheet. These time scales can be captured with a simple argument inspired by the motion of a wrinkle in a carpet resting on ground. Indeed, since the excess length in the concave sector relative to contact with the container is $\ell = \pi R \epsilon^2$, with $\epsilon = d/R$ being the strength of the d cone, the sheet materially rotates by an angle ℓ/R when the bump completes a rotation. As a consequence, the material rotation is at frequency $f_r = \phi \epsilon^2/2$ if the concave sector rotates at a frequency ϕ . These quantities being not constant, we take a temporal average $f_r = \langle \phi(t) \epsilon_s(t)^2/2 \rangle$, where ϵ_s is the time-dependent strength of the d cone. Because of the parametric coupling, $\langle \phi \rangle = f/2$. Besides, from Fig. 4, rotation occurs mostly when the center displacement is smaller than d , i.e., during half a period of forcing. During that half period, $t \in (\pi/f, 2\pi/f)$, $\phi \simeq f$ so that we average the time-dependent d cone strength $\epsilon_s(t) = \epsilon[1 + d_F/d \sin(2\pi s f t)]$, which yields

$$f_r = \frac{1}{4} f \epsilon^2 \left[1 - \frac{4}{\pi} \frac{d_F}{d} + \frac{1}{2} \left(\frac{d_F}{d} \right)^2 \right], \quad (1)$$

and provides a good fit to the experimental data in Fig. 5 if the prefactor is left free.

Developable modes.—Now we discuss the possible modes of vibration. The sound velocity is $c = (E/\rho)^{1/2}$ so that the typical frequencies for stretching and bending modes are $f_s \sim c/R_s$ and $f_b \sim hc/R_s^2$, respectively (R_s is the radius of the sheet), and which ratio $f_s/f_b \sim R_s/h \gg 1$, so that only bending oscillations are possible at low frequencies, for which stretching follows adiabatically bending. Hence we expect only developable modes to be excited and restrict to a d cone with tip located at the pushing finger. Its shape is given by the transverse displacement $w(r, \theta, t) = r g(\theta, t)$ in polar coordinates (r, θ) . The developability constraint can be written as [1,3]

$$\int (g^2 - g'^2) d\theta = 0. \quad (2)$$

Adding the kinetic energy $(\partial w/\partial t)^2$ to the bending energy

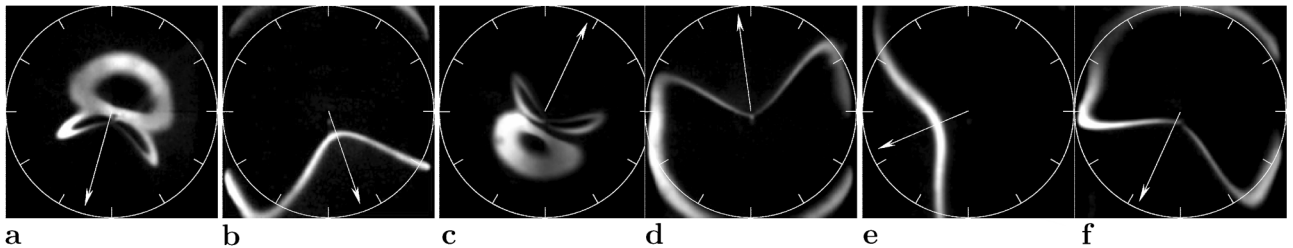


FIG. 4. Counterclockwise rotation at velocity $f/2$ in the ROT tongue. Center displacement, $d = 4$ mm, forcing amplitude $d_F = 3$ mm, and frequency $f = 11$ Hz. The reflection of a fluorescent ring is seen; it is approximately circular in the convex sector of the d cone and inverted in the concave part (axis marked by an arrow). The rotation velocity $\phi(t)$ and the amplitude of the d cone $\epsilon_s(t)$ vary along a period of rotation. (a) $t = 0$. Concave sector pointing to 6:30, high amplitude ϵ_s , slow rotation. (b) $t = 16$ ms, medium ϵ_s , fast rotation. (c) $t = 56$ ms, high ϵ_s , slow rotation. (d) $t = 74$ ms, medium ϵ_s , fast rotation. (e) $t = 92$ ms, small ϵ_s , very fast rotation; note that the shape is slightly asymmetric at fast rotation. (f) $t = 106$ ms, medium ϵ_s , slow rotation.

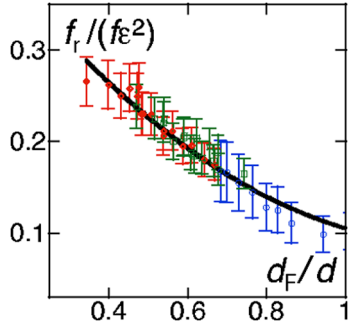


FIG. 5 (color online). Frequency of material rotation f_r normalized with frequency of forcing f and d cone strength $\epsilon = d/R$, vs amplitude of forcing d_F over center displacement d . $d = 3$ mm (\circ), $d = 4$ mm (\square), and $d = 5.9$ mm (\diamond). Fit to equation $f_r = p/4f\epsilon^2[1 - 4/\pi(d_F/d) + (d_F/d)^2/2]$, yielding $p = 1.86$.

(proportional to the square of the curvature), the dynamical equation is easily obtained as

$$\frac{\partial^2 g}{\partial t^2} = -\frac{4 \ln(R_s/R_c)}{\rho h R_s^4} \left\{ [B(\theta) + \lambda] \left(g + \frac{\partial^2 g}{\partial \theta^2} \right) + \frac{\partial^2}{\partial \theta^2} \left[B(\theta) \left(g + \frac{\partial^2 g}{\partial \theta^2} \right) \right] \right\}, \quad (3)$$

where λ is a Lagrange multiplier corresponding to the constraint of developability and the logarithmic dependence has a cutoff due to size of the d cone core R_c . The mass per unit surface is $\rho h = 0.137$ kg/m². The bending modulus $B = Eh^3/12(1 - \nu^2)$ may have a dependence in the polar angle θ to account for the anisotropy of the sheet. In the case of constant B , the static solution $g_0(\theta)$ was given by [3]; the Lagrange multiplier is then $\lambda \simeq 13.5B$. The vibration modes can be determined by a small perturbation around the static solution, $g = g_0 + \delta g$, with the boundary conditions $\delta g(\pm\theta_1) = \partial_\theta \delta g(\pm\theta_1) = 0$. For constant B only an asymmetrical modulation of the concave sector is possible, the lowest frequency corresponding to a tilt mode TM for which the resonant frequency is $\nu_1 = \sqrt{(B + \lambda) \ln(R_s/R_c) / \rho h / R_s^2} / \pi \simeq 13.6$ Hz, for our values (we take $R_c \simeq 2$ cm), which is close to the measured ν_1 [Fig. 3(a)].

On the other hand, a rolling mode, RM, exists because the sheet used here, being anisotropic, has two preferential axes along which bending stiffness is maximum and minimum, respectively. In our case, the anisotropy of our plate can be represented as $B(\theta) = B_m + \Delta B \cos 2\theta$, with $B_m = 4.3 \times 10^{-4}$ N · m and $\Delta B = 9 \times 10^{-5}$ N · m. Since bending is energetically more expensive along the maximum axis, the concave region of the d cone tends to roll towards one of the minima of bending energy, allowing two preferential angular positions of the structure. Thus, each minimum admits oscillations of the concave region of the

d cone, at a well-defined frequency, the restoring force being determined by the angular gradient of bending energy. Rough estimates for the frequency of the RM in our case give $\nu_0 \sim (\Delta B/B)^{1/2} \nu_1 \sim 6$ Hz, which is of the order of $f_0/2$, f_0 being the minimum of the ROT tongue [Fig. 3(a)], consistently with a parametric rotation.

Conclusion.—We reported the first observation of the bending modes of a d cone structure when submitted to a parametric forcing. In particular, the motion of a d cone concave sector by external vibration exhibits common features with particle motion in fluctuating potential [16,17]. In our case, although the modulated potential is symmetric, the presence of inertia provides the kinetic energy to overcome the bending energy barrier.

The collaborative research was supported by ECOS-CONICYT under Project No. C03E04 and FONDAP Project No. 11980002, and by ANR Blanc OPADETO. A. B. is grateful to Mokhtar Adda-Bedia for discussions about wrinkles in carpets.

-
- [1] M. Ben Amar and Y. Pomeau, Proc. R. Soc. A **453**, 729 (1997).
 - [2] S. Chaïeb, F. Melo, and J-C. Géminard, Phys. Rev. Lett. **80**, 2354 (1998).
 - [3] E. Cerda and L. Mahadevan, Phys. Rev. Lett. **80**, 2358 (1998).
 - [4] T. A. Witten, Europhys. Lett. **23**, 51 (1993).
 - [5] A. E. Lobkovsky and T. A. Witten, Phys. Rev. E **55**, 1577 (1997).
 - [6] A. E. Lobkovsky, S. Gentges, H. Li, D. Morse, and T. A. Witten, Science **270**, 1482 (1995).
 - [7] E. Sultan and A. Boudaoud, Phys. Rev. Lett. **96**, 136103 (2006).
 - [8] G. During, Ch. Jossierand, and S. Rica, Phys. Rev. Lett. **97**, 025503 (2006).
 - [9] E. M. Kramer and A. E. Lobkovsky, Phys. Rev. E **53**, 1465 (1996).
 - [10] P. A. Houle and J. P. Sethna, Phys. Rev. E **54**, 278 (1996), vibration trapping A.
 - [11] A. Gopinathan, T. Witten, and V. Venkataramani, Phys. Rev. E **65**, 036613 (2002).
 - [12] E. Cerda, S. Chaïeb, F. Melo, and L. Mahadevan, Nature (London) **401**, 46 (1999).
 - [13] A. Boudaoud, P. Patricio, Y. Couder, and M. Ben Amar, Nature (London) **407**, 718 (2000).
 - [14] E. Hamm, B. Roman, and F. Melo, Phys. Rev. E **70**, 026607 (2004).
 - [15] T. H. Heaton, Phys. Earth Planet. Inter. **64**, 1 (1990).
 - [16] F. Jlicher *et al.*, Rev. Mod. Phys. **69**, 1269 (1997).
 - [17] Y. Couder *et al.*, Nature (London) **437**, 208 (2005).
 - [18] See for instance, S. Douady and S. Fauve, Europhys. Lett. **6**, 221 (1988).